

Nuclear spin polarization transfer across an organic-semiconductor interface

Lucas Goehring^{a)} and Carl A. Michal^{b)}

Department of Physics and Astronomy, University of British Columbia, 6224 Agricultural Road, Vancouver, British Columbia, V6T 1Z1, Canada

(Received 11 June 2003; accepted 19 August 2003)

Motivated by Tycko's proposal to harness optically pumped nuclear spin polarization for the enhancement of nuclear magnetic resonance (NMR) signals from biological macromolecules, we investigate the transfer of thermal nuclear spin polarization between ^1H or ^{19}F in an organic overlayer and ^{31}P at the surface of micron-sized InP particles by Hartmann–Hahn cross polarization. Comparison with analytic and numerical models indicates that the total quantity of polarization transferred across the semiconductor-organic interface is limited by the relatively short room-temperature ^1H $T_{1\rho}$ (11 ms) and the slow diffusion of nuclear spin polarization in the semiconductor. Models and spin-counting experiments indicate that we are able to transfer approximately 20% of the total nuclear spin polarization originating in the organic overlayer to the semiconductor, supporting the feasibility of transferred optically pumped NMR. © 2003 American Institute of Physics. [DOI: 10.1063/1.1617975]

I. INTRODUCTION

Nuclear magnetic resonance (NMR) is an extremely powerful technique for the study of a wide variety of materials, especially biological macromolecules.^{1–3} Perhaps its greatest weakness, however, is sensitivity. In thermal equilibrium at room temperature, in a strong laboratory magnetic field, the net polarization of the nuclear spins is often less than 1 in 10^5 . Typically 10^{16} – 10^{18} copies of each molecule are necessary for meaningful structural measurements.^{4,5} For some types of biological samples, such as membrane-bound proteins or large antibody-receptor complexes, this quantity may be prohibitively large.

One avenue of increasing the sensitivity and thereby reducing the sample size requirement is enhancing the feeble equilibrium nuclear spin polarization by optical pumping, whereby angular momentum from circularly polarized photons is transferred to electronic and nuclear spins. In order to harness optical pumping as a general NMR signal enhancement technique, the nuclear spin polarization so produced must be transferred to the species of interest. It has been shown that nuclear spin polarization in optically pumped noble gases may be transferred to other nuclear spins in liquids⁶ and on the surface of solids.^{7,8} Tycko has proposed⁵ that nonequilibrium nuclear spin polarization, generated within a semiconductor by optical pumping, may be transferred to an organic or biological sample of interest on the surface. This procedure, which has not yet been demonstrated, has been given the name transferred optically-pumped NMR (TOPNMR).

While optical pumping in high-magnetic field has been

most studied in GaAs,^{9–14} it has been pointed out⁵ that GaAs is unlikely to be a good substrate for TOPNMR because the abundant nuclear spins in GaAs have quadrupole moments. No quadrupole splittings are observed in unstrained GaAs because of the cubic symmetry, but nuclei at sites near the surface are likely to experience large electric field gradients and large quadrupole splittings, hindering the transfer of polarization across the interface. As an alternative, InP was suggested because ^{31}P is 100% abundant, spin-1/2, and has a relatively large gyromagnetic ratio. Results of optical pumping studies in InP have been encouraging,^{5,15–17} and will guide attempts to demonstrate and apply TOPNMR.

A key ingredient of TOPNMR is the efficient transfer of nuclear spin polarization from the semiconductor substrate to the surface species. It has been suggested that spin polarization densities of at least 5% of the optically pumped source polarization must be obtained in the target nuclei⁵ to make the method feasible. Tomaselli *et al.*¹⁸ have demonstrated the transfer of nuclear spin polarization from ^1H in trioctylphosphine oxide (TOPO) caps to ^{31}P in InP nanocrystals. In that work a number of surface environments were distinguished, but no estimate of the efficiency of polarization transfer was reported. In this work, we present cross-polarization experiments demonstrating the transfer of nuclear spin-polarization between ^{31}P in micron-sized InP particles and ^1H and ^{19}F in surface-bound para-trifluoromethylbenzyl-ether (TFMBE). By modeling of the flow of nuclear spin polarization from the ^1H rich surface layer into the bulk InP, we show that spin diffusion combined with the relatively short ^1H rotating frame relaxation time ($T_{1\rho}$) limits the total amount of spin polarization that may be transferred to approximately 20% of the total at room temperature. Transfer in the other direction, from semiconductor to overlayer, is also demonstrated with similar efficiency. We begin by describing simple analytic and numerical models for spin-polarization transport near the

^{a)}Current address: Department of Physics, University of Toronto, Toronto, Ontario, Canada.

^{b)}Author to whom all correspondence should be addressed; electronic mail: michal@physics.ubc.ca

organic/semiconductor interface that we then compare to experimental results.

II. SPIN DIFFUSION

The Hamiltonian of a system of nuclear spins in a strong magnetic field can be written as the sum of a Zeeman coupling of the nuclear magnetic moments to the field, $H_Z = \hbar \sum_i \omega_i I_{zi}$, in which I_{zi} is the z component of angular momentum for the i th spin and $\omega_i/2\pi$ is its resonance frequency, along with the truncated homonuclear dipole couplings, $H_D = \hbar \sum_{i < j} d_{ij} (I_{zi} I_{zj} - \frac{1}{4} (I_{i+} I_{j-} + I_{i-} I_{j+}))$,¹⁹ in which d_{ij} is the dipolar coupling between spins i and j . For a many-spin system, the detailed evolution produced by this Hamiltonian rapidly becomes intractable, however Bloembergen²⁰ suggested that the $I_{i+} I_{j-} + I_{i-} I_{j+}$ flip-flop terms of H_D can lead to the spatial motion of nuclear spin polarization. In many cases, this motion is well described by a diffusion equation,^{20–22} $\rho_t = D \nabla^2 \rho$, in which D is a diffusion coefficient and ρ represents the nuclear spin polarization density. D is related to the dipolar coupling strength, d_{ij} , and can be written

$$D = c \frac{\gamma^2 \hbar \sqrt{I(I+1)}}{r}, \quad (1)$$

where γ is the nuclear gyromagnetic ratio, r is the nearest-neighbor distance,^{23–25} and c is a constant of order unity that depends on details including the symmetry of the lattice and the direction of the magnetization gradient. Calculations of c based on a variety of methods have been performed,^{23,25–28} and a relatively precise experimental determination of D in CaF_2 has recently been reported.²⁹

The spin diffusion we wish to model occurs during Hartmann–Hahn cross polarization (CP),³⁰ used to connect ^1H in the surface species to ^{31}P in the substrate. Under such continuous rf irradiation, d_{ij} and D are scaled by $(3 \cos^2 \theta - 1)/2$, where θ is the angle between the static and effective magnetic fields.^{19,21,31} For on-resonance irradiation, d_{ij} and D are effectively halved.

We model the flow of polarization from a thin ^1H rich surface layer into a semi-infinite ^{31}P substrate with a modified one-dimensional diffusion equation:

$$\rho_t = D \rho_{xx} - \frac{\rho}{T_{1\rho}}, \quad (2)$$

where relaxation effects are included with the $\rho/T_{1\rho}$ term. Our models include separate values of $T_{1\rho}$ in the substrate and overlayer, but ignore the more complicated changes in $T_{1\rho}$ that likely occur near the interface.

In order to find an analytic solution, we take $T_{1\rho}$ in the substrate to be infinite (a reasonable approximation as the ^{31}P $T_{1\rho}$ is much longer than the CP contact times used), and approximate relaxation effects in the surface layer with the boundary condition

$$\rho(0,t) = \rho_0 e^{-t/T_{1\rho}}. \quad (3)$$

This is a reasonable approximation for short CP times, when little of the initial spin polarization has moved into the substrate.

For this analytic model, we take the overlayer as infinitely thin, and impose the initial condition $\rho(x,0) = 0$ on $0 < x < \infty$. The one-dimensional diffusion equation with boundary condition Eq. (3) can be solved with Laplace transforms to yield

$$\rho(x,t) = \rho_0 \int_0^t \frac{x}{2\lambda \sqrt{\pi\lambda D}} e^{-(t-\lambda)/T_{1\rho}^H} e^{-x^2/4D\lambda} d\lambda. \quad (4)$$

After integrating over $0 < x < \infty$, we find the total nuclear spin polarization that has diffused into the sample is given by

$$P(t) = \epsilon A \rho_0 \sqrt{DT_{1\rho}^H} e^{-t/T_{1\rho}^H} \text{erfi}(\sqrt{t/T_{1\rho}^H}) \quad (5)$$

in which ϵ is the fractional surface coverage, A is the surface area of the sample, and $\text{erfi}(x)$ is the imaginary error function, given by $-i \text{erf}(ix)$. For short times, $P(t) \propto \sqrt{t}$.

This model fails to take into account the depletion of the ^1H polarization by its diffusion into the bulk InP. This limitation is overcome by numerically integrating Eq. (2) in a one-dimensional model consisting of an initially polarized 6-Å-thick ^1H rich layer on top of a 90-Å-thick initially unpolarized layer. This numerical model includes relaxation in both the surface layer and bulk, and has been incorporated into a nonlinear least-squares fitting routine.³²

III. EXPERIMENTAL METHODS

A TFMBE coated InP powder was prepared by grinding pieces of undoped InP (99.999%, Aldrich, Milwaukee, WI) with a mortar and pestle for 15 min inside a nitrogen filled glove bag (to prevent oxidation of the freshly exposed surface). The powder was then added to a solution of 0.5 M 4-trifluoromethylbenzylbromine (TFMBB) (98%, Aldrich, Milwaukee, WI) in acetonitrile (ACS Reagent grade, Sigma, St. Louis, MO) and held for 3 h at 60 °C to allow the TFMBB to react with the InP surface. Reaction with TFMBB is known to leave persistently attached TFMBE^{33,34} on the phosphorus rich (111)B surface of cleaved InP^{33,34} single crystals. The binding of the methylene carbon is thought to be through residual –OH functionalities on the InP surface.³⁴ The powder was then washed four times with neat acetonitrile to remove any unbound TFMBB and then dried in air. 186 mg of the sample were used for NMR experiments, while the remaining ~100 mg was used for surface area measurements. A control sample was prepared similarly, but without the addition of TFMBB.

Surface area measurements were made using Micromeritics ASAP 2000 and Coulter LS particle size analyzers on portions of the powder samples suspended in water. Surface area estimates were derived from the measured particle size distributions assuming spherical particles.

NMR spectra were acquired at room temperature using a Varian Unity/Inova 400 NMR spectrometer at 9.4 T with a Varian/Chemagnetics T3 triple resonance probe with 4-mm-diam coil. rf power levels were adjusted for Hartmann–Hahn match with typical $\nu_1 = 55$ –60 kHz.

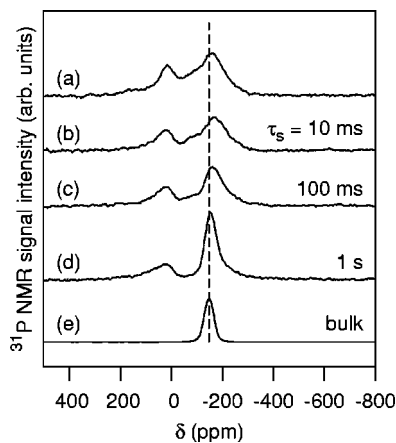


FIG. 1. ^{31}P NMR signals from TFMBE-coated InP. (a) Signal from surface ^{31}P acquired with CP from ^1H . (b), (c), and (d) Signal acquired with CP followed by a longitudinal storage with storage time indicated. (e) Signal from ^{31}P in the bulk arising from single pulse excitation. All spectra apodized with 1 kHz full-width at half-maximum exponential broadening before Fourier transformation. The vertical line is a guide to the eye.

IV. RESULTS AND DISCUSSION

A ^{31}P NMR spectrum acquired from the surface of a TFMBE coated InP powder with Hartmann–Hahn cross polarization from ^1H is displayed in Fig. 1(a). The NMR spectrum from the surface of the InP particles differs in several respects from that arising from the bulk, [Fig. 1(e), acquired with single pulse excitation]. Most strikingly, the surface signal is split into two resolved peaks, one near the bulk InP peak, and a second downfield at ~ 20 ppm. In addition, the upfield peak is both shifted and broadened compared to the bulk.

Tomaselli *et al.* demonstrated the existence of several distinct ^{31}P sites on the surface of TOPO capped InP quantum dots.¹⁸ In that work, peaks at $\delta = -118$ and -199 ppm were assigned to surface sites of the InP, while peaks with δ between -8 and 71 ppm were assigned to the TOPO caps. In our spectra, we see similar changes in the bulk InP line shape, qualitatively consistent with the surface sites as described in that work. In our samples, there is no phosphorus in the capping molecules, and thus we cannot assign the downfield portion of the spectrum to capping sites. Rather, we assign the broad peak near 20 ppm to phosphorus in oxides on the surface of our particles.

To reinforce this interpretation of the spectra, a pair of ^{31}P $\pi/2$ pulses separated by a variable storage delay, τ_s , was appended to the CP sequence to store the ^{31}P nuclear spin polarization along the magnetic field and allow spin diffusion to carry it away from the particle surface and into the bulk. Because the spin diffusion during τ_s occurs in the absence of any rf fields, this period is not described by the above-developed models, in particular, the nuclear spin polarization is confined to the InP, and ^1H in the surface species play no role (except possibly to shorten the T_1 of ^{31}P in close proximity to the interface). The ^{31}P NMR signals acquired with this pulse sequence are displayed in Figs. 1(b), 1(c), and 1(d). As τ_s is increased, the intensity of the downfield peak decreases while the intensity of the upfield peak increases, its

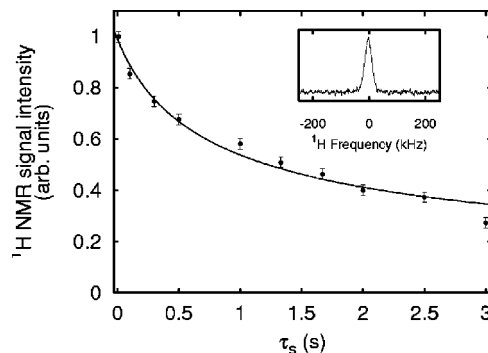


FIG. 2. Integrated intensity of ^1H spectra vs longitudinal storage time for $^1\text{H} \rightarrow ^{31}\text{P} \rightarrow ^1\text{H}$ double CP experiments. The storage delay allows spin diffusion to reduce the surface spin polarization density of the ^{31}P . The solid line is a best fit explained in the text. The inset shows the proton spectrum corresponding to the first data point.

line shape approaches that of the bulk, and the overall spectral intensity remains approximately constant (reflecting the long ^{31}P T_1 of ~ 300 s).

An alternative view of the effect of the storage delay was obtained by following the storage period with a second CP, and then acquiring the ^1H signal. The signals observed (inset of Fig. 2) represent nuclear spin polarization that originated in the ^1H at the surface, was transferred to the ^{31}P and allowed to evolve for τ_s before being transferred back to ^1H at the surface. If the polarization were well localized at the interface following CP, spin diffusion would spread it into the bulk with a Gaussian profile having a depth $\ell \propto \sqrt{\tau_s}$ and an amplitude at the surface $\propto 1/\sqrt{\tau_s}$. If, however, polarization were initially spread into the bulk (with a Gaussian profile), as expected from the initial cross polarization step, subsequent evolution would appear unchanged, but with a shift of the time axis related to the initial depth. The dependence of signal intensity observed as a function of τ_s is shown, along with a best fit to $C/\sqrt{\tau_s + \tau_0}$, in Fig. 2. A straightforward interpretation of the best fit value of τ_0 , 0.4 s, in terms of the initial polarization depth, using $\ell = \sqrt{4D\tau_0/\pi}$ and $D = 2.9 \times 10^{-18}$ m^2/s , the origin of which is described below, yields a characteristic depth of $\ell = 12$ \AA , somewhat deeper than the single lattice constant (5.9 \AA) that we would expect to become polarized during the short $\tau_{\text{CP}} = 1$ ms used. It is likely, however, that spin diffusion is inhibited near the surface during τ_s due to poor resonance overlap from one ^{31}P site to the next.²² This slow spin diffusion manifests itself as a greater than expected τ_0 . Our estimate of D should be valid when the rf is turned on however, because the chemical shift differences responsible for the poor overlap are irrelevant in the presence of the spin-lock field.

In order to measure the maximum quantity of nuclear spin polarization transferred from the ^1H at the surface into the ^{31}P inside the InP particles, the dependence of the ^{31}P NMR signal intensity was measured as a function of τ_{CP} .

The dependence of the signal intensity with contact time is shown in Fig. 3 along with curves representing the analytic [Eq. (5)], and numerical models. The only adjustable parameter in the analytic model is an overall scaling parameter, which has been adjusted here for the best fit at short τ_{CP} .

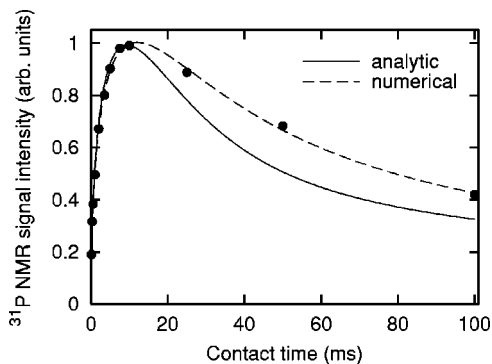


FIG. 3. Integrated intensity of cross polarized ^{31}P spectra as a function of τ_{CP} with best fits to the analytic model, Eq. (5), and numerical simulation.

The value of the ^1H $T_{1\rho}$ used is that found by inserting a variable length ^1H spin-lock period between the ^1H $\pi/2$ pulse and the CP period, 11 ms. This model does an excellent job of describing the initial build-up of polarization, but, as expected, fails at longer τ_{CP} due to the approximation made at the boundary.

The curve shown representing the numerical model is a best fit allowing the variation of separate spin diffusion constants and $T_{1\rho}$ values in the ^1H rich and InP layers, along with an overall scaling parameter. The spin diffusion constant for ^{31}P in InP, D_{P} , from the fitting routine is $3.2 \times 10^{-18} \text{ m}^2/\text{s}$, in good agreement with our best estimate of $2.9 \times 10^{-18} \text{ m}^2/\text{s}$, which is based on $\bar{D}[111]$ from Ref. 27. Our estimate includes a factor of 0.1, based on Fig. 4 of Ref. 27 in order to account for the presence of the In nuclear spins, whose presence will suppress spin diffusion, as well as the factor of 1/2 mentioned earlier to account for the presence of the on-resonance rf field. The same fit provides $D_{\text{H}} = 6.7 \times 10^{-17} \text{ m}^2/\text{s}$, which is somewhat lower than would be expected from a straightforward estimate based on an H–H nearest-neighbor distance of 2.5 \AA ($\sim 3 \times 10^{-16} \text{ m}^2/\text{s}$), but the presence of the ^{19}F nuclear spins and the asymmetric environment of ^1H will likely slow spin diffusion in the ^1H rich layer. Because our model also makes no attempt to account for the interface itself, any impediment to spin diffusion caused by the interface may be included by the fit in D_{H} . This point is considered further below. The value of the ^1H $T_{1\rho}$ from the fit, 15 ms, is in qualitative agreement with the 11 ms measured directly. Finally, the fit ^{31}P $T_{1\rho}$, 700 ms is consistent with experimental measurements made with a ^{31}P spin-lock inserted following the CP period which indicate a ^{31}P $T_{1\rho} \gg 100 \text{ ms}$.

Our numerical model makes no explicit reference to the detailed nature of the interface. Assuming the TFMBE is linked through bridging oxygens, as concluded in Ref. 34, we would expect ^1H – ^{31}P distances of $\sim 3.6 \text{ \AA}$, providing ^1H – ^{31}P dipolar couplings of $\sim 1000 \text{ Hz}$, very similar in magnitude to the ^{31}P – ^{31}P couplings in InP. For a perfect interface this would actually yield a slightly greater spin diffusion coefficient at the interface than found in the bulk, as the diffusion coefficient scales as $d_{ij} \times r^2$ and the H–P distance at the interface is greater than the P–P nearest neighbor distance in the bulk. A rough interface or patchy surface

coverage of the TFMBE would produce bottlenecks that could be absorbed into our fit values of D_{H} .

Our goal is to estimate the portion of the initial ^1H nuclear spin polarization that crosses the interface into the InP particles. The numerical simulations indicate that approximately 20% of the nuclear spin polarization initially present in the ^1H rich layer is transferred into the InP. To find an experimental estimate, we begin with an estimation of the total number of TFMBE ligands in the sample as found from a $^1\text{H} \rightarrow ^{19}\text{F}$ cross-polarization experiment, compared to the ^{19}F signal acquired with single pulse experiment on a poly(tetrafluoroethylene) sample. Accounting for the finite size of the ^1H spin reservoir (six ^1H for each three ^{19}F on each TFMBE ligand), we find a total of 1.8×10^{17} TFMBE ligands in our 186 mg sample. We expect this cross-polarization experiment to provide nearly quantitative results, as the ^1H and ^{19}F are strongly coupled so that the cross-polarization time (2.5 ms) is short compared to the $T_{1\rho}$'s, and because the ligands are attached to macroscopic particles so that no large scale molecular motions interfere with the couplings. Here, the CP experiment is necessary because of probe background signals for both ^1H and ^{19}F .

Next, a $^{19}\text{F} \rightarrow ^1\text{H} \rightarrow ^{31}\text{P}$ double-CP experiment, calibrated with the InP signal from a single-pulse experiment on the same sample allowed to fully relax, suggests 3.7×10^{16} TFMBE ligands (again accounting for the finite sizes of the ^1H and ^{19}F reservoirs). Employing the 1.8×10^{17} ligands found from the $^1\text{H} \rightarrow ^{19}\text{F}$ experiment, we again find a 20% efficiency for moving polarization from the ^1H layer into InP, in agreement with the numerical simulations. The excellent agreement of the experiment and simulation suggests that all of the TFMBE ligands in the sample are tightly coupled to ^{31}P in the InP particles, and that it is the slow spin diffusion within the semiconductor, combined with the quick ^1H $T_{1\rho}$ that limits the total polarization transferred across the organic/semiconductor interface.

The ultimate success of TOPNMR depends on the reverse of this process: polarization must be moved from the semiconductor to the overlayer. In principle, we could simply transfer polarization from ^{31}P to ^1H in order to quantify the efficiency of this process, however the long ^{31}P T_1 makes this impractical. By comparing the amplitude of the ^1H signal observed in the $^1\text{H} \rightarrow ^{31}\text{P} \rightarrow ^1\text{H}$ experiments shown in Fig. 2 with that from an adamantane standard, we find that we are able to transfer approximately 14% of the polarization that had been moved into the InP back into the surface layer, with a 1 ms contact time. This experiment underestimates the amount of polarization transferable from semiconductor to overlayer because some of the polarization transferred to the surface of the InP is lost by diffusion into the bulk and is not available for return to the overlayer.

Results from the particle size analyzers suggest a powder surface area on the order of $0.3 \text{ m}^2/\text{g}$. Scanning electron microscope images showed highly irregularly shaped InP particles ranging from 0.5 to $100 \text{ }\mu\text{m}$ in diameter, in qualitative agreement with the distributions found from the particle size analyzers. With some variation depending on the orientation, a smooth InP surface exposes about 10^{15} lattice sites per cm^2 . Assuming 1/3 of these are occupied with TFMBE (so

that the TFMBE number density is similar to that in liquid TFMBB), we expect to find at most 2×10^{17} ligands on the surface. The agreement of this estimate with that from the above-given NMR measurements is fortuitous, as it is known that TFMBB does not react with the In rich (111)A face of single crystal InP,^{33,34} so it seems unlikely that we could have achieved close to 100% coverage.

Additional evidence that our surface area estimate is low, likely due to the rough, irregular shapes of our particles, comes from the intensities of $^1\text{H} \rightarrow ^{31}\text{P}$ cross-polarization experiments (e.g., Fig. 3), which suggest a factor of 4.5 more protons on the surface. This excess signal could arise from residual $-\text{OH}$ groups attached to lattice sites in between the TFMBE ligands (which were assumed to only occupy 1/3 of the sites) as well as from oxides on faces of the particles with which the TFMBB did not react. The excellent fit of the simulation to the data of Fig. 3 reflects the fact that the model is insensitive to whether the ^1H polarization originated in surface $-\text{OH}$ or in TFMBE. Our simulations show little sensitivity to the thickness of the ^1H rich layer (except for overall scale), as expected because spin diffusion in the ^1H rich layer is much faster than in the bulk.

A similar suite of experiments was performed on the control sample prepared without TFMBB. A similar mass of sample resulted in about 75% of the signal intensity from $^1\text{H} \rightarrow ^{31}\text{P}$ CP experiments under the same experimental conditions. No signal was observed in $^1\text{H} \rightarrow ^{19}\text{F}$ or $^{19}\text{F} \rightarrow ^1\text{H} \rightarrow ^{31}\text{P}$ experiments. All of the NMR results are consistent with a total of about 2×10^{17} TFMBE ligands on the sample prepared with TFMBB, covering approximately 10%–20% of the surface, with the remaining surface containing ^1H in oxides.

V. CONCLUSIONS

Tycko suggested that for TOPNMR to be effective, spin polarization densities of at least 5% of the source polarization must be obtained in the target nuclei. Comparison of $^1\text{H} \rightarrow ^{19}\text{F}$, $^{19}\text{F} \rightarrow ^1\text{H} \rightarrow ^{31}\text{P}$, and $^1\text{H} \rightarrow ^{31}\text{P}$ CP experiments indicate that we have been able to transfer about 20% of the initial ^1H nuclear spin polarization originating in a thin organic layer into the semiconductor, consistent with numerical modeling. Transfer of a portion of this polarization back into the organic surface layer has also been demonstrated with comparable efficiency. At low temperatures, relevant for TOPNMR experiments, we expect these efficiencies can be increased considerably as the ^1H rotating frame relaxation slows. These results are encouraging for efforts toward TOPNMR.

ACKNOWLEDGMENTS

This work was supported by the Natural Sciences and Engineering Research Council of Canada. The Varian NMR

spectrometer was purchased with the assistance of the Canada Foundation for Innovations and the British Columbia Knowledge Development Fund. We thank Allan Bertram, Jerry Bretherton, Michael Eastwood, George Englezos, Isaac Leung, and David Perrin for help with particle size measurement and Victor Chen and Andre Marziali for help in obtaining SEM images. L.G. thanks Iain Taylor for a critical reading of an early draft.

- ¹ Wüthrich, *NMR of Proteins and Nucleic Acids* (Wiley, New York, 1986).
- ² V. Kanelis, J. D. Forman-Kay, and L. E. Kay, *IUBMB Life* **52**, 291 (2001).
- ³ S. R. Kiihne and H. J. M. de Groot, *Perspectives on Solid State NMR in Biology* (Kluwer Academic, Norwell, MA, 2001).
- ⁴ C. P. Slichter, *Annu. Rev. Phys. Chem.* **37**, 25 (1986).
- ⁵ R. Tycko, *Solid State Nucl. Magn. Reson.* **11**, 1 (1998).
- ⁶ H. C. Gaede, Y.-Q. Song, R. E. Taylor, E. J. Munson, J. A. Reimer, and A. Pines, *Appl. Magn. Reson.* **8**, 373 (1995).
- ⁷ C. Bowers, H. W. Long, T. Pietrass, H. C. Gaede, and A. Pines, *Chem. Phys. Lett.* **205**, 168 (1993).
- ⁸ G. Navon, Y.-Q. Song, T. Room, S. Appelt, R. E. Taylor, and A. Pines, *Science* **271**, 1848 (1996).
- ⁹ D. Paget, *Phys. Rev. B* **24**, 3776 (1981).
- ¹⁰ D. Paget, *Phys. Rev. B* **25**, 4444 (1982).
- ¹¹ S. K. Buratto, D. N. Shykind, and D. P. Weitekamp, *J. Vac. Sci. Technol. B* **10**, 1740 (1992).
- ¹² S. E. Barrett, R. Tycko, L. N. Pfeiffer, and K. W. West, *Phys. Rev. Lett.* **72**, 1368 (1994).
- ¹³ R. Tycko, S. E. Barrett, G. Dabbagh, L. Pfeiffer, and K. W. West, *Science* **268**, 1460 (1995).
- ¹⁴ T. Pietrass, A. Bifone, T. Rööm, and E. L. Hahn, *Phys. Rev. B* **53**, 4428 (1996).
- ¹⁵ C. A. Michal and R. Tycko, *Phys. Rev. Lett.* **81**, 3988 (1998).
- ¹⁶ C. A. Michal and R. Tycko, *Phys. Rev. B* **60**, 8672 (1999).
- ¹⁷ A. Patel, O. Pasquet, J. Bharatam, E. Hughes, and C. R. Bowers, *Phys. Rev. B* **60**, R5105 (1999).
- ¹⁸ M. Tomaselli, J. L. Yarger, M. Bruchez, R. H. Havlin, D. DeGraw, A. Pines, and A. P. Alivisatos, *J. Chem. Phys.* **110**, 8861 (1999).
- ¹⁹ C. P. Slichter, *Principles of Magnetic Resonance* (Harper and Row, New York, 1963).
- ²⁰ N. Bloembergen, *Physica (Utrecht)* **15**, 386 (1949).
- ²¹ B. H. Meier, *Adv. Magn. Opt. Reson.* **18**, 1 (1994).
- ²² A. Z. Genack and A. G. Redfield, *Phys. Rev. B* **12**, 78 (1975).
- ²³ I. J. Lowe and S. Gade, *Phys. Rev.* **156**, 817 (1967).
- ²⁴ A. G. Redfield, *Phys. Rev.* **116**, 315 (1959).
- ²⁵ A. G. Redfield and W. N. Yu, *Phys. Rev.* **169**, 443 (1968).
- ²⁶ P. Borckmans and D. Walgraef, *Phys. Rev.* **167**, 282 (1968).
- ²⁷ C. Tang and J. S. Waugh, *Phys. Rev. B* **45**, 748 (1992).
- ²⁸ B. Cowan, W. J. Mullin, and E. Nelson, *J. Low Temp. Phys.* **77**, 181 (1989).
- ²⁹ W. Zhang and D. G. Cory, *Phys. Rev. Lett.* **80**, 1324 (1998).
- ³⁰ S. R. Hartmann and E. L. Hahn, *Phys. Rev.* **128**, 2042 (1962).
- ³¹ S. M. de Paul, M. Tomaselli, and A. Pines, *J. Chem. Phys.* **108**, 826 (1998).
- ³² J. E. Dennis, D. M. Gay, and R. E. Welsch, *ACM Trans. Math. Softw.* **7**, 369 (1981).
- ³³ A. M. Spool, K. A. Daube, T. E. Mallouk, J. A. Belmont, and M. S. Wrighton, *J. Am. Chem. Soc.* **108**, 3155 (1986).
- ³⁴ M. Sturzenegger and N. S. Lewis, *J. Am. Chem. Soc.* **118**, 3045 (1996).